Photoinjector drive laser of the FLASH FEL

Ingo Will,[1,*] Horst I. Templin,[1] Siegfried Schreiber,[2] and Wolfgang Sandner[1]

[1]*Max-Born-Institute for Nonlinear Optics and Short Pulse Spectroscopy, Berlin, Germany*
[2]*Deutsches Elektronen-Synchrotron, Hamburg, Germany*
[*]*will@mbi-berlin.de*

Abstract: The upgraded photoinjector drive laser of the free-electron laser facility FLASH at DESY Hamburg is described in this paper. This laser produces trains of 800 and 2400 ultraviolet picosecond pulses at 1 MHz and 3 MHz repetition rate in the trains, respectively. The amplifying elements of the system are Nd:YLF-rods, which are pumped by fiber-coupled semiconductor diodes. Compared to the flashlamp-pumped photocathode laser previously used at FLASH, the new diode-pumped laser features a better reliability and a significantly improved stability of its pulse parameters.

OCIS codes: (140.4050) Mode-locked lasers; (140.3530) Lasers, neodymium; (140.2600) Free-electron lasers (FELs).

References and links

1. W. Ackermann, G. Asova, V. Ayvazyan, A. Azima, N. Baboi, J. Bähr, V. Balandin, B. Beutner, A. Brandt, A. Bolzmann, R. Brinkmann, O. I. Brovko, M. Castellano, P. Castro, L. Catani, E. Chiadroni, S. Choroba, A. Cianchi, J. T. Costello, D. Cubaynes, J. Dardis, W. Decking, H. Delsim-Hashemi, A. Delserieys, G. Di Pirro, M. Dohlus, S. Düsterer, A. Eckhardt, H. T. Edwards, B. Faatz, J. Feldhaus, K. Flöttmann, J. Frisch, L. Fröhlich, T. Garvey, U. Gensch, C. Gerth, M. Görler, N. Golubeva, H.-J. Grabosch, M. Grecki, O. Grimm, K. Hacker, U. Hahn, J. H. Han, K. Honkavaara, T. Hott, M. Hüning, Y. Ivanisenko, E. Jaeschke, W. Jalmuzna, T. Jezynski, R. Kammering, V. Katalev, K. Kavanagh, E. T. Kennedy, S. Khodyachykh, K. Klose, V. Kocharyan, M. Körfer, M. Kollewe, W. Koprek, S. Korepanov, D. Kostin, M. Krassilnikov, G. Kube, M. Kuhlmann, C. L. S. Lewis, L. Lilje, T. Limberg, D. Lipka, F. Löhl, H. Luna, M. Luong, M. Martins, M. Meyer, P. Michelato, V. Miltchev, W. D. Möller, L. Monaco, W. F. O. Müller, O. Napieralski, O. Napoly, P. Nicolosi, D. Nölle, T. Nuñez, A. Oppelt, C. Pagani, R. Paparella, N. Pchalek, J. Pedregosa-Gutierrez, B. Petersen, B. Petrosyan, G. Petrosyan, L. Petrosyan, J. Pflüger, E. Plönjes, L. Poletto, K. Pozniak, E. Prat, D. Proch, P. Pucyk, P. Radcliffe, H. Redlin, K. Rehlich, M. Richter, M. Roehrs, J. Roensch, R. Romaniuk, M. Ross, J. Rossbach, V. Rybnikov, M. Sachwitz, E. L. Saldin, W. Sandner, H. Schlarb, B. Schmidt, M. Schmitz, P. Schmüser, J. R. Schneider, E. A. Schneidmiller, S. Schnepp, S. Schreiber, M. Seidel, D. Sertore, A. V. Shabunov, C. Simon, S. Simrock, E. Sombrowski, A. A. Sorokin, P. Spanknebel, R. Spesyvtsev, L. Staykov, B. Steffen, F. Stephan, F. Stulle, H. Thom, K. Tiedtke, M. Tischer, S. Toleikis, R. Treusch, D. Trines, I. Tsakov, E. Vogel, T. Weiland, H. Weise, M. Wellhöfer, M. Wendt, I. Will, A. Winter, K. Wittenburg, W. Wurth, P. Yeates, M. V. Yurkov, I. Zagorodnov, and K. Zapfe, "Operation of a free-electron laser from the extreme ultraviolet to the water window," Nat. Photonics **1**(6), 336–342 (2007).
2. R. Akre, D. Dowell, P. Emma, J. Frisch, S. Gilevich, G. Hays, P. Hering, R. Iverson, C. Limborg-Deprey, H. Loos, A. Miahnahri, J. Schmerge, J. Turner, J. Welch, W. White, and J. Wu, "Commissioning the Linac Coherent Light Source injector," in *Phys. Rev. ST Accel. Beams* (2008), p. 030703.
3. S. D. Mitri, E. Allaria, L. Badano, C. Bontoiu, M. Cornacchia, P. Craievich, M. Danailov, G. D. Ninno, B. Diviacco, O. Ferrando, S. Ferry, F. Iazzourene, S. V. Milton, G. Penco, S. Spampinati, M. Trovo, M. Veronese, W. Fawley, S. Lidia, G. Penn, J. Qiang, K. G. Sonnad, M. Venturini, R. Warnock, A. A. Zholents, I. V. Pogorelov, M. Borland, G. Bassi, J. A. Ellison, K. Heinemann, R. Fiorito, A. Shkvarunets, and J. C. Tobin, "Design and simulation challenges for FERMI@elettra," Nucl. Instrum. Methods 19–27 (2009).
4. A. Cianchi, D. Alesini, A. Bacci, M. Bellaveglia, R. Boni, M. Boscolo, M. Castellano, L. Catani, E. Chiadroni, S. Cialdi, A. Clozza, L. Cultrera, G. Di Pirro, A. Drago, A. Esposito, M. Ferrario, L. Ficcadenti, D. Filippetto, V. Fusco, A. Gallo, G. Gatti, A. Ghigo, L. Giannessi, C. Ligi, M. Mattioli, M. Migliorati, A. Mostacci, P. Musumeci, E. Pace, L. Palumbo, L. Pellegrino, M. Petrarca, M. Preger, M. Quattromini, R. Ricci, C. Ronsivalle, J. Rosenzweig, A. Rossi, C. Sanelli, L. Serafini, M. Serio, F. Sgamma, B. Spataro, F. Tazzioli, S. Tomassini, C. Vaccarezza, M. Vescovi, and C. Vicario, "High brightness electron beam emittance evolution measurements in an rf photoinjector," Phys. Rev. ST Accel. Beams **11**(3), 032801 (2008).

#153463 - $15.00 USD Received 25 Aug 2011; revised 16 Oct 2011; accepted 21 Oct 2011; published 8 Nov 2011

5. S. Rimjaem, G. Asova, J. W. Bähr, C. Boulware, K. Boyanov, K. Flöttmann, H. J. Grabosch, L. Hakobyan, M. Hänel, Y. Ivanisenko, S. Khodyachykh, S. Korepanov, M. Krasilnikov, S. Lederer, A. Oppelt, B. Petrosyan, D. Richter, S. Riemann, J. Rönsch, K. Rosbach, A. Shapovalov, L. Staykov, and F. Stephan, "Status and perspectives of the PITZ facility upgrade," in *Proceedings of FEL 2007, Novosibirsk, Russia* (2007), pp. 354–357.
6. Y. Muroya, M. Lin, T. Watanabe, G. Wu, T. Kobayashi, K. Yoshii, T. Ueda, M. Uesaka, and Y. Katsumura, "Ultra-fast pulse radiolysis system combined with a laser photocathode RF gun and a femtosecond laser," Nucl. Instr. Meth. Res. Sect. A: Accel. Spectrom. Detect. Assoc. Equip. **489**(1-3), 554–562 (2002).
7. J. Belloni, H. Monard, F. Gobert, J.-P. Larbre, A. Demarque, V. D. Waele, I. Lampre, J.-L. Marignier, M. Mostafavi, J. C. Bourdon, M. Bernard, H. Borie, T. Garvey, B. Jacquemard, B. Leblond, P. Lepercq, M. Omeich, M. Roch, J. Rodier, and R. Roux, "ELYSE—A picosecond electron accelerator for pulse radiolysis research," Nucl. Instr. Meth. Res. Sect. A: Accel. Spectrom. Detect. Assoc. Equip. **539**(3), 527–539 (2005).
8. J. Rosenzweig, S. Anderson, K. Bishofberger, X. Ding, A. Murokh, C. Pellegrini, H. Suk, A. Tremaine, C. Clayton, C. Joshi, K. Marsh, and P. Muggli, "The Neptune photoinjector," Nucl. Instr. Meth. Res. Sect. A: Accel. Spectrom. Detect. Assoc. Equip. **410**(3), 437–451 (1998).
9. P. Musumeci, J. T. Moody, R. J. England, J. B. Rosenzweig, and T. Tran, "Experimental generation and characterization of uniformly filled ellipsoidal electron-beam distributions," Phys. Rev. Lett. **100**(24), 244801 (2008).
10. S. Schreiber, S. Lederer, P. Michelato, L. Monaco, D. Sertore, and J. H. Han, "Cathode issues at the FLASH photoinjector," in *Proceedings of FEL08, Gyeongju, Korea* (2008), pp. 552–555.
11. I. Will, G. Koss, and I. Templin, "The upgraded photocathode laser of the TESLA Test Facility," Nucl. Instr. Meth. Res. Sect. A: Accel. Spectrom. Detect. Assoc. Equip. **541**(3), 467–477 (2005).
12. I. Will, A. Liero, D. Mertins, and W. Sandner, "Feedback-Stabilized Nd:YLF Amplifier System for Generation of Picosecond Pulse Trains of an Exactly Rectangular Envelope," IEEE J. Quantum Electron. **34**(10), 2020–2028 (1998).
13. N. J. Walker, V. Ayvazyan, L. Froehlich, M. Grecki, S. Schreiber, J. Carwardine, B. Chase, M. Davidsaver, T. Matsumoto, and S. Michizono, "Operation of the FLASH Linac with long bunch trains and high average current," in *Proceedings of PAC09, Vancouver, BC, Canada* (2009), pp. 2766–2768.
14. M. Altarelli, R. Brinkmann, M. Chergui, W. Decking, B. Dobson, S. Düsterer, G. Grübel, W. Graeff, H. Graafsma, J. Hajdu, J. Marangos, J. Pflüger, H. Redlin, D. Riley, I. Robinson, J. Rossbach, A. Schwarz, K. Tiedtke, T. Tschentscher, I. Vartaniants, H. Wabnitz, H. Weise, R. Wichmann, K. Witte, A. Wolf, M. Wulff, and M. Yurkov, "The European X-Ray Free-Electron Laser technical design report," Techn. Rep. DESY 2006–097 (DESY, 2006).
15. I. Will and G. Klemz, "Generation of flat-top picosecond pulses by coherent pulse stacking in a multicrystal birefringent filter," Opt. Express **16**(19), 14922–14937 (2008).
16. J. T. Hunt, J. A. Glaze, W. W. Simmons, and P. A. Renard, "Suppression of self-focusing through low-pass spatial filtering and relay imaging," Appl. Opt. **17**(13), 2053–2057 (1978).
17. L. Froehlich, A. Hamdi, M. Luong, J. Novo, M. Goerler, P. Goettlicher, D. Noelle, D. Pugachov, H. Schlarb, S. Schreiber, M. Staack, and M. Werner, "First operation of the FLASH machine protection system with long bunch trains," in *Proceedings of LINAC 2006, Knoxville, Tennessee USA*, 2006), pp. 262–264.
18. DESY, "DOOCS, the Distributed Object Oriented Control System," http://tesla.desy.de/doocs/.
19. J. Yang, F. Sakai, T. Yanagida, M. Yorozu, Y. Okada, K. Takasago, A. Endo, A. Yada, and M. Washio, "Low-emittance electron-beam generation with laser pulse shaping in photocathode radio-frequency gun," J. Appl. Phys. **92**(3), 1608 (2002).
20. I. Will, "Generation of flattop picosecond pulses by means of a two-stage birefringent filter," Nucl. Instr. Meth. Res. Sect. A: Accel. Spectrom. Detect. Assoc. Equip. **594**(2), 119–125 (2008).

1. Introduction

Photo injectors became a proven tool for generation of high-density, high brightness electron bunches in the past two decades. Today they are often exploited as the initial electron source for short-wavelength free electron lasers (FELs) [1–5]. Photo injectors are also used as electron sources in accelerators for radiation chemistry [6]. They also provide electron beams for pulsed radiolysis experiments [7], for plasma beat wave experiments [8], or for fundamental accelerator research [9].

Radio frequency (RF) photo injectors contain a photocathode positioned at the backplane of the first half cell of an RF cavity. The cathode is illuminated with pulses from the so-called drive laser generating bunches of electrons by photo emission. An intense electric field of several ten MV/m accelerates the electron bunches. Strong acceleration is required to mitigate degradation of emittance of these bunches due to space charge effects.

The pulse parameters of the drive laser determine the basic properties of the electron bunches produced by the photo injector, such as their sequence in time, their duration or the

#153463 - $15.00 USD Received 25 Aug 2011; revised 16 Oct 2011; accepted 21 Oct 2011; published 8 Nov 2011

amount of bunch charge. In addition, this laser has influence on the more qualitative properties of the electron bunches, which are often of particular importance for the desired application. This regards, for example, the stability of the produced charge and its synchronization accuracy to the RF of the photo injector or the linac, as well as the emittance of the electron bunches. In short, the drive laser is a crucial device that has a strong impact on several important parameters of the electron bunches generated by the photoinjector.

In the following chapter, we will discuss the specific features of the photoinjector drive laser for FLASH and the demands on this laser in detail.

2. Desired pulse parameters of the photoinjector drive laser for FLASH

FLASH is the free-electron user facility at DESY, Hamburg, operating in the VUV and soft X-ray wavelength range [1]. The FLASH electron source is an RF gun based photo injector [5]. It uses a high efficient Cs_2Te photocathode to produce the initial electron bunches, which are further accelerated in a superconducting linac of the TESLA type. For efficient emission of electron bunches, this photocathode material requires UV pulses of λ ~260 to 270 nm in wavelength, which must be provided by the drive laser [10].

The quantum efficiency of Cs_2Te cathodes is between 5 and 10% with a lifetime of more than 100 days of operation [10]. Since this efficiency is sensitive to the vacuum pressure, a considerable safety margin of 10 in the available laser pulse energy is advised. An additional factor of 10 is needed to compensate for losses by experimental optical arrangements, e.g. pulse shapers. In summary, the laser should provide about 30 μJ energy per pulse in order to produce electron bunches with a charge of 3 nC, the maximum charge to be generated at FLASH.

The longitudinal shape of the laser pulses is important in two aspects. It influences space-charge induced emittance growth of the electron bunches, and also their compression process later in the accelerator. In order to keep space-charge effects small, the drive laser should produce pulses with duration between 10 and 20 ps.

An important advantage of superconducting linacs is the efficient acceleration of particles with high duty cycle. At FLASH, bunch trains of up to 800 μs length with hundreds or thousands of individual pulses can be accelerated in the so-called burst mode at a repetition rate of 10 Hz. Therefore, the drive laser must also generate bursts of laser pulses. A burst contains up to 800 individual picosecond long pulses (micropulses) with 1 MHz repetition rate. In a second, enhanced mode the linac is operated with 3 MHz repetition rate and with up to 2400 micropulses in the burst. Stable operation of the laser with 3 MHz bursts is a precondition for making this new operational mode available to the users of FLASH.

Since the photoinjector drive laser influences several important properties of the electron beam significantly, this laser must generally work in a very stable manner during the experimental runs. Several Photoinjector drive lasers have been successfully operated since 1997 at FLASH [11,12]. However, it was often difficult to meet the reliability requirements. Since these lasers contained flashlamps as pump sources in their amplifiers, they suffered limited lifetime of these flashlamps. An acceptable reliability of these lasers was reached by exchanging all flashlamps regularly, typically once per month. The downtime of FLASH caused by the laser was 0.6%, compared to a total FLASH downtime of 7%. This has been an acceptable performance so far. However, in the present running periods, the repetition rate of the accelerator has been increased from 5 to 10 Hz. Simultaneously, the goal was to reduce the downtime by at least a factor of two.

To solve the problems resulting from the ageing of the flashlamps, we had to eliminate these lamps completely and pump the laser amplifiers by semiconductor diodes. However, it turned out that very special pump diodes were required for the FLASH photoinjector drive laser. These diodes must reach a power of several 100 W and generate fairly long pulses of up to 2 ms duration. Suitable laser diodes, which reach a long lifetime despite of the periodic thermal shock in this mode, became available only in the last years.

#153463 - $15.00 USD Received 25 Aug 2011; revised 16 Oct 2011; accepted 21 Oct 2011; published 8 Nov 2011

The new laser system, which is described in this paper, has been tested and systematically improved during the past years. The first version of the completely diode-pumped photocathode laser was developed at the MBI and installed at the Photo Injector Test Facility at DESY Zeuthen (PITZ) in 2005. This laser has been used for operating the PITZ RF gun from 2005 to 2007 with 1 MHz repetition rate in the pulse trains. When the enhanced operational mode with 3 MHz repetition rate was planned for FLASH at Hamburg in 2009, we developed new Pockels cell drivers that support the generation of long pulse trains with 3 MHz repetition rate in the trains. In addition, we increased the output power of the laser by improving the optical scheme of the amplifiers and by using more powerful pump diodes.

With the enlarged repetition rate and output power, the new laser was installed and successfully operated during the full beamloading experiment at FLASH in 2009 [13]. After these experiments, it was decided to set up a second laser at FLASH identical with the first one to support further development work. In future, we intend to increase the average power of this laser and its repetition rate in the bursts to 4.5 MHz to fit the specification of the photoinjector drive laser for the upcoming European XFEL [14].

3. Layout of the laser

The photoinjector drive laser, whose optical layout is shown in Fig. 1, contains the following main building blocks:

- the laser oscillator,
- a chain of six amplifier stages A1…A6,
- two Pockels cells PC1 and PC2 that are integrated into the amplifier chain,
- the wavelength converter,
- a variable attenuator,
- optics to image the ultraviolet pulses to the photocathode,
- a computerized control system.

Figure 2 shows the generation of the desired output pulse trains by the interplay of these parts. This figure also illustrates the role of the pulse-selecting Pockels cells. At first, the laser oscillator produces the initial pulses with 54.16 MHz repetition rate. These pulses are synchronized to the high-frequency accelerating field in the cavities of the linac with sub-picosecond accuracy. Secondly, the Pockels cell PC1 selects intermediate trains of 1.2 ms length with 1 or 3 MHz repetition rate from the initial pulse train of the oscillator. After amplification in the amplifier stages A1…A4, the Pockels cell PC2 picks the final pulse pattern from the intermediate pulse train. These pulses are then further amplified in the power amplifiers A5 and A6. A wavelength conversion stage converts the infrared (IR) pulses from the laser amplifier to the ultraviolet (UV). After adjusting their energy with a variable attenuator, the UV pulses are finally projected on to the photocathode of the photo injector by proper imaging optics. A control computer allows for feedback stabilization and for remote control of the individual components of the laser.

We describe the function and the construction of the most important building blocks of the laser in more detail in the following sections.

#153463 - $15.00 USD Received 25 Aug 2011; revised 16 Oct 2011; accepted 21 Oct 2011; published 8 Nov 2011

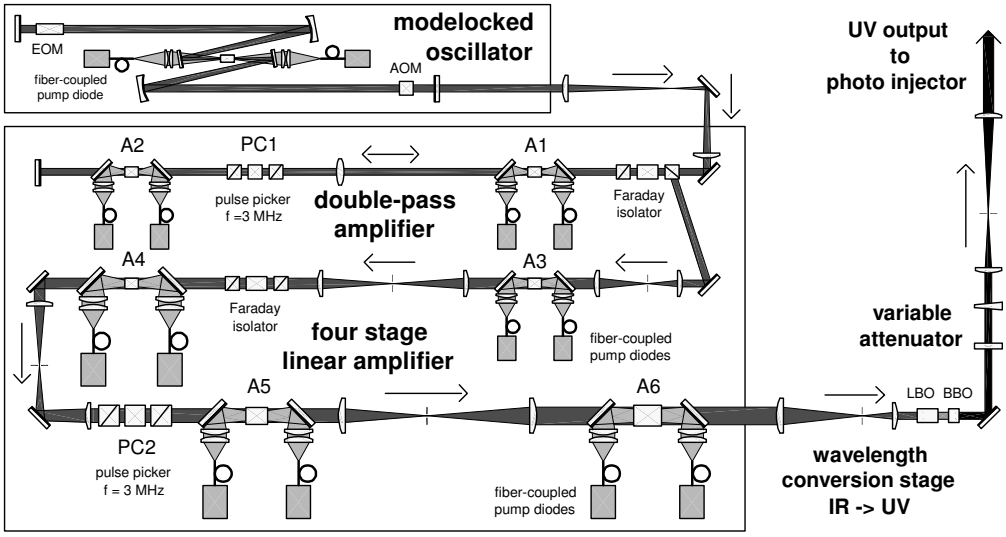

Fig. 1. Optical layout of the photoinjector drive laser

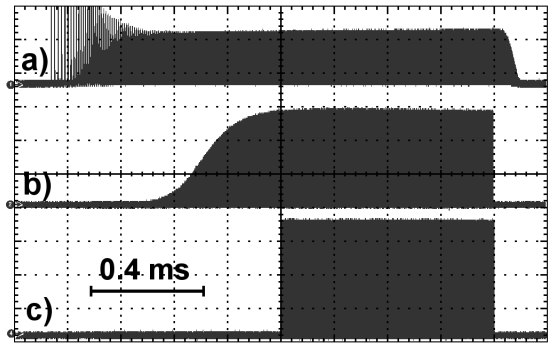

Fig. 2. Pulse trains measured at different places in the laser system: a) Initial pulse train produced by the laser oscillator, b) intermediate pulse train behind the preamplifier (measured after amplifier stage A4), c) output pulse train of the final amplifier (measured after the power amplifier A6).

4. Main building blocks of the laser

4.1. The laser oscillator

The oscillator generates the initial picosecond laser pulses with a temporal spacing of 18.5 ns. Thus the round-trip frequency in the resonator of the oscillator amounts to 54.17 MHz, which is the 24th subharmonics of 1.3 GHz, the operation frequency of the FLASH linac.

A 16 mm long Nd:YLF rod that is end-pumped by two fiber-coupled diodes of 25 W peak power serves as the lasing element of the oscillator. In order to form picosecond pulses, the laser oscillator contains two active modelockers in its cavity. These modelockers are driven by RF signals of 27.08 and 650 MHz frequency, respectively. Operating the fast 650 MHz phase modulator alone would cause twelve individual pulses traveling in the resonator (so-called harmonic modelocking). The slower acousto-optic modelocker, which modulates the gain of the resonator with the second harmonics of its drive frequency, selects only one of these pulses. Thus the use of two modelockers allows for generation of picosecond pulses of 18 ps duration (FWHM).

#153463 - $15.00 USD Received 25 Aug 2011; revised 16 Oct 2011; accepted 21 Oct 2011; published 8 Nov 2011

To produce these pulses in a stable manner, the round-trip frequency of the laser oscillator must exactly match the modulation frequency of the amplitude modulator. Therefore the resonator length is constantly adjusted in such a manner that the initial relaxation oscillations in the pulse train of the oscillator settle after ~1 ms (Fig. 2, upper trace). This is accomplished by means of a control computer, which continuously records the pulse trains of the oscillator with an ADC. In dependence on the envelope of the pulse train, this computer controls a Piezo actuator that moves one of the mirrors of the resonator appropriately. The oscillator produces pulse trains with an undisturbed, flat portion of > 2 ms duration this way.

In addition to the stable generation of picosecond pulses, the described active-modelocking technique also ensures a reliable synchronization between the produced laser pulses and the accelerating RF field of the photo injector. By optically cross-correlating the pulses from two laser oscillators we have found that the pulse jitter is below 0.1 ps rms, even in the presence of mechanical disturbance, for example due to vibrating vacuum pumps. This synchronization accuracy is by far sufficient for reliable operation of the RF gun and the linac.

Besides the new oscillator described above, the oscillators previously used at TESLA Test Facility, FLASH and PITZ [11,15] was used to generate the initial picosecond pulses for the new laser system as well. This oscillator type has a two times longer resonator, resulting in a round-trip frequency of 27.16 MHz. Therefore stable generation of single picosecond pulses requires three modelockers in the oscillator cavity. These modelockers are driven by RF signals of 13.54, 108.66 and 1300 MHz frequency respectively. Since the highest modulation frequency amounts to 1300 MHz, the produced pulses have 12 to 15 ps duration (fwhm) and are slightly shorter than the pulses from the new oscillator described above.

The pulse duration obtained with both the new and the old oscillators fulfill the requirements of the FLASH linac. It turned out that the new oscillator with shorter resonator is easier to handle than the old one. In particular, it needs only two phase-stable RF driving signals, since it contains only two modulators. Furthermore, it features a higher stability due to the reduced resonator length. Therefore the new oscillator is, in general, more suitable for seeding the amplifier, except for the cases when UV output pulses shorter than 13 ps have to be generated by the laser system.

4.2. The amplifier chain

The amplifier chain raises the energy of the picosecond pulses by more than four orders of magnitude. It fits in a housing of 1.8x0.5x0.16 m size and includes four spatial filters, two Pockels cells with their drivers, two Faraday isolators and six gain modules (Fig. 3). To reach the needed amplification, the first two gain modules are used in double-pass. Thus it takes eight passes through the individual gain modules to increase the energy of the weak input laser pulses to their final output energy.

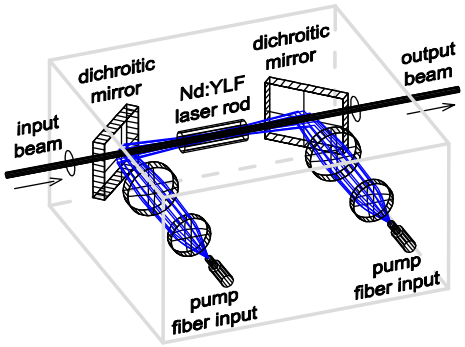

Fig. 3. Scheme of the compact gain modules contained in the amplifier chain.

#153463 - $15.00 USD Received 25 Aug 2011; revised 16 Oct 2011; accepted 21 Oct 2011; published 8 Nov 2011

Each of the gain modules contains a 16 mm long Nd:YLF laser rod of 5 mm diameter. They are water-cooled and pumped by two fiber-coupled laser diodes of 805 nm wavelength. The pump diodes of the first three modules reach 100 W peak power, whereas diodes of 200 W peak power are used for pumping the three final amplifier stages. Transport of the radiation from the diodes to the gain modules is accomplished by 4 to 6 m long fibers with 400 µm core diameter. These fibers allowed us to mount all pump diodes with their power supplies in a standard 20-inch rack beside the laser table.

Separating the optical setup of the laser from its electrical parts has several advantages. Most importantly, changing laser diodes does not require any realignment of the optical setup of the amplifier any more. Thus pumping the Nd:YLF rods with fiber-coupled pump diodes was an important design decision, which allowed us to build a compact and easy-to-maintain amplifier chain.

The so-called relay-imaging technique [16] was applied in the last four amplifier stages to preserve a stable beam profile during the long pulse trains. Therefore these amplifier stages contain telescopes, which successively image the laser beam profile from each gain module into the following one. Simultaneously, the telescopes expand the laser beam to the desired diameter. This technique was already used in other burst-mode lasers [12] to reduce the undesirable effect of thermally induced perturbation of the refraction index in the laser rods on the beam profile ("thermal lensing"). Apart from that, the telescopes act as spatial filters due to pinholes in the focus of the lenses. They clean the laser beam from intensity peaks that result from imperfections of the optical elements and from diffraction at small dust particles on the optical surfaces. Thus the spatial filters improve the quality of the amplified laser beam significantly.

When passing through the amplifier chain, the laser beam is enlarged to 3.5 mm diameter before the final amplifier. The magnification of the individual telescopes was chosen in such a manner that the intensity of the laser beam does not exceed 0.1 GW/cm^2 in the laser rods and thus allowing the laser to operate in a non-cleanroom environment.

In summary, the amplifier chain was optimized to support a stable long-term operation of the laser with good beam quality in a standard laboratory environment.

4.3. The wavelength converter

The wavelength converter transfers the infrared (IR) pulses from the laser system with 1047 nm wavelength to ultraviolet (UV) pulses. The latter have a wavelength of 262 nm, which is needed for efficient operation of the Cesium Telluride cathodes in the RF photo injector.

The actual conversion process takes place in an 8 mm long LBO crystal that generates the green second harmonics of the infrared laser radiation, followed by a 6 mm long BBO crystal that transfers this green radiation to the UV. Both crystals are mounted in temperature-controlled housings and can be remotely tilted for precise adjustment of the phase-matching angle. A de-magnifying telescope located at the output of the amplifier reduces the diameter of the beam to ~1.2 mm and adapts the intensity of the infrared pulses from the laser to the intensity needed for optimum wavelength conversion in the LBO and BBO crystals. With this arrangement, the maximum conversion efficiency obtained from the IR to the UV amounts to 16%.

The wavelength converter is followed by an attenuator, which consists of a half-wave retardation plate and a UV polarizer. Rotating this plate remotely leads to a modification of the polarization state of the UV pulses and therefore changes the portion of the UV pulses that is transmitted by the final UV polarizer. This arrangement is used to tune the energy of the UV sent to the photocathode and to adjust the bunch charge emitted by the RF photo injector. It allows operating both the laser amplifier and the wavelength converter at a constant power level independently on the bunch charge required by the linac. This is beneficial for stable operation of the laser system.

#153463 - $15.00 USD Received 25 Aug 2011; revised 16 Oct 2011; accepted 21 Oct 2011; published 8 Nov 2011

5. Performance and limits of the laser

The pulse trains at the output of the amplifier chain measured after amplifier A6 for 3 MHz and for 1 MHz repetition rate in the trains are shown in Fig. 4. They were recorded with a standard silicon photodiode of 2 ns resolution and a digital oscilloscope of 2 GHz bandwidth. These measurements were taken at a current in the pump diodes of I_{pump} = 40 A. The total energy of the pulse trains was 224 mJ and 218 mJ at f = 3 MHz and f = 1 MHz, respectively.

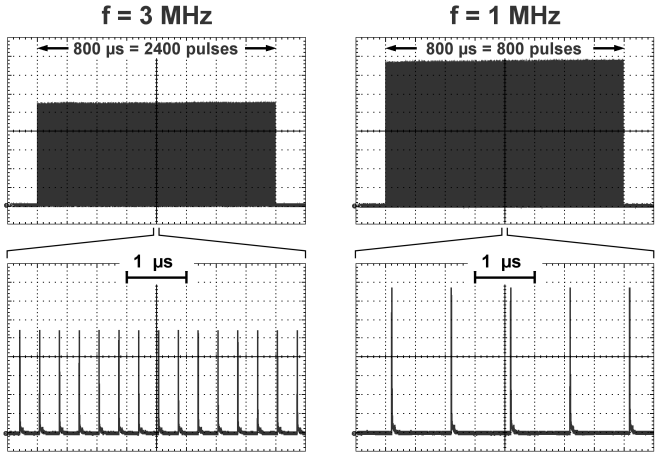

Fig. 4. Output pulse train of the Nd:YLF amplifier chain measured after the final amplifier A6 for 3 MHz and for 1 MHz repetition rate in the trains. The vertical scale in the left oscilloscope traces is two times smaller than the scale in the right traces. Therefore the amplitude of the pulses measured at f = 1 MHz is about three times larger than the amplitude at f = 3 MHz repetition rate in the train.

In the following paragraphs we give some details on the pulse energy and the duration of the micropulses in the train. Firstly, we summarize the parameters of the infrared pulses directly produced by the laser. Subsequently, we discuss the same pulse parameters, but after conversion to the ultraviolet.

Figure 5 shows the energy of the infrared micropulses in the trains measured after the final amplifier A6, plotted in dependence on the current through the pump diodes. As one can expect, the pulse energy rises linearly with increasing pump power. For a pump current of I_{pump} = 44 A, this energy is 310 µJ compared to 108 µJ at 3 MHz repetition rate.

The energy of the amplified IR pulses is nearly three times larger at 1 MHz than at 3 MHz repetition rate in the train, which is simply a consequence of strong saturation of the average laser power in the final amplifiers. This also means that the total energy in the 800 µs long pulse trains is nearly independent of the repetition rate ($E_{total,\ train}$ = 0.25 J at f = 1 MHz, compared to E_{train} = 0.26 J at f = 3 MHz, both measured at I_{pump} = 44 A). The observed strong saturation of the final amplifiers is generally beneficial, since it favors stable operation of the laser system. As a result, the fluctuation of the energy of the individual micropulses of the train is smaller than 0.5% (rms value) at the output of the amplifier chain.

The saturation of the average power in the amplifiers is a relatively slow process, which has a time scale of several tens of microseconds [12]. That is why this saturation mechanism does not affect the pulse shape or the actual duration of the individual micropulses in the trains. We have measured the duration of the IR pulses from the oscillator and at the output of the amplifier chain with a scanning autocorrelator (Fig. 6). Within the accuracy of our measurement, the pulse duration measured after the amplifier is identical to the pulse duration of the oscillator. In addition, the duration of the IR pulses does not depend on the output power and the pulse energy of the laser.

#153463 - $15.00 USD Received 25 Aug 2011; revised 16 Oct 2011; accepted 21 Oct 2011; published 8 Nov 2011

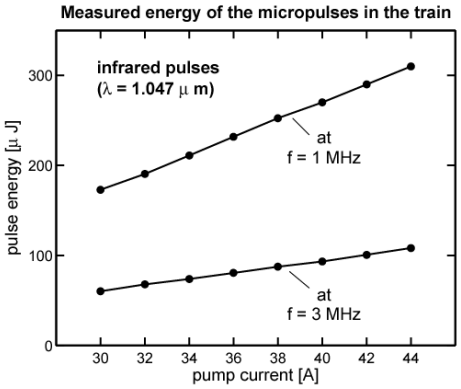

Fig. 5. Energy of the infrared micropulses in the train in dependence on the current of the amplifier pump diodes. The pulse energy was measured after amplifier A6.

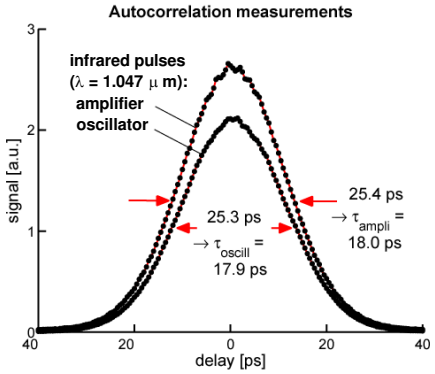

Fig. 6. Duration of the infrared pulse of the oscillator and of the output of the laser amplifier, measured by a scanning SHG autocorrelator.

Next, we compare the parameters of the infrared pulses to pulse parameters obtained after conversion to the ultraviolet. As already pointed out, this conversion takes place in two nonlinear crystals, both in conjunction generating the fourth harmonics of the infrared pulses of the laser.

A plot of the energy of the UV pulses in dependence on the current in the pump diodes of the amplifiers is presented in Fig. 7. For the 3 MHz operational modes, pulses of up to 13 μJ energy are generated. This is sufficient for producing 3 nC bunch charge and 9 mA average beam at the current RF photo injector at FLASH. For the 1 MHz operational modes, UV pulse trains with up to 40 μJ pulse energy per individual micropulse are produced. The observed gain in pulse energy is not only due to the higher energy in the IR, but also due to a better conversion efficiency of the UV converter at 1 MHz repetition rate. We typically measure an efficiency of the UV conversion process between 8 and 12% at 3 MHz, while we reach 13 to 16% at 1 MHz repetition rate.

It turns out that the energy of the IR pulses not only determines the efficiency of the UV converter, but also has some influence on the shape of the produced UV pulses. To illustrate this effect, Fig. 8 presents measurements of the shape of the UV pulses with a synchroscan streak camera with 2 ps temporal resolution (model Optoscope SC10 produced by Optronis, Germany). The main result of these measurements is that the conversion process shortens the pulses from τ_{IR} = 17.9 ps in the IR to τ_{UV} = 13.1 ps in the UV for moderate pulse energy (E_{UV} = 12 μJ). This is simply due to the fourth order nonlinearity of the conversion process: The laser radiation is less effectively converted at the edges of the pulse than at its maximum, which leads to the observed pulse shortening. At higher pulse energy (E_{UV} = 31 μJ) on the

#153463 - $15.00 USD Received 25 Aug 2011; revised 16 Oct 2011; accepted 21 Oct 2011; published 8 Nov 2011

other hand, the instantaneous conversion efficiency saturates at the peak of the pulse (Fig. 8). We see that the peak is somewhat less efficiently converted than the edges of the pulse, which results in pulse lengthening to 18.4 ps (FWHM) and in a slight modification of the initially Gaussian pulse shape.

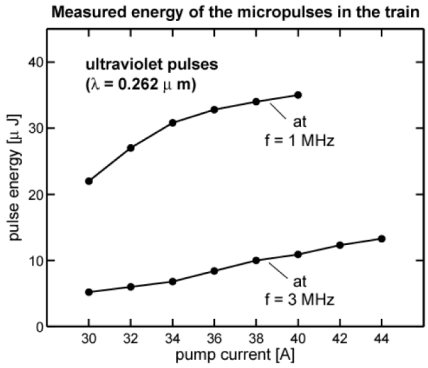

Fig. 7. Energy of the UV micropulses of the train after the wavelength converter in dependence on the current of the pump diodes of the amplifiers

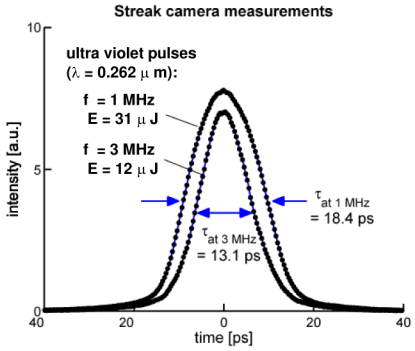

Fig. 8. UV output pulses measured with a synchroscan streak camera

To sum up, the effective duration of the UV output pulse is determined by the balance between two effects:

- pulse shortening due to the nonlinearity of the wavelength conversion process and
- pulse lengthening due to saturation of this process.

Unlike saturation in the laser amplifiers, both effects taking place in the wavelength converter act on a picosecond time scale. Therefore, they lead to a measurable change of the pulse duration and of the pulse shape itself in dependence on the instantaneous laser intensity in the frequency conversion crystals.

When using the laser for driving a photo injector, we typically operate the laser with a current of 42 A for 3 MHz repetition rate, thus producing trains of 13 ps long UV with 12 μJ energy. In the 1 MHz mode, we usually reduce the current to 30 A. This leads to pulses of ~22 μJ energy and of 17 ps duration. In both cases, the produced pulse energy is sufficient for generating bunches of up to 3 nC charge with the Cesium Telluride photocathodes presently used in the FLASH photo injector.

#153463 - $15.00 USD Received 25 Aug 2011; revised 16 Oct 2011; accepted 21 Oct 2011; published 8 Nov 2011

Table 1. Pulse parameters of the photocathode laser.

Parameter	value	
	at f = 3 MHz ("lower-energy" mode)	at f = 1 MHz ("higher-energy" mode)
Time structure of the laser output	trains of picosecond pulses	
Shape of the individual pulses of the train	nearly Gaussian	
Output wavelength	262 nm (UV)	
Length of the pulse trains	0…800 µs (programmable)	
Temporal spacing between the micropulses	0.33 µs	1.0 µs (programmable)
Number of pulses per train	1…2400 (programmable)	1…800 (programmable)
Duration (FWHM) of the micropulses (with the 54 MHz oscillator)	13 ps	15…19 ps
Available energy of the individual pulses in the trains	13 µJ	36 µJ
Available energy of the whole UV train	32 mJ	29 mJ
Synchronization accuracy to the RF of the linac	$\sigma < 1$ ps	
Repetition rate	5 trains/sec	10 trains/sec

Table 1 summarizes the pulse parameters typically obtained for the two main operational modes of the laser at the FLASH linac.

An important feature of the laser is its flexibility with regard to the micro-pulse repetition rate. For certain user experiments, larger bunch spacing is required. A FPGA based controller is used to provide an easy interface for the operators to change the bunch spacing by acting on the 2nd Pockels cell. Within the base frequency of the FLASH timing system of 9.03 MHz, the intra-train spacing can be chosen freely. Often bunch spacings of 2 µs (500 kHz) or 10 µs (100 kHz) are requested by the experiments.

Since the controller acts on a fast Pockels cell, it also serves as an interface between the machine protection system and the laser. Depending on machine operating conditions or component failures, the controller is able to block the Pockels cell within 3 µs thus inhibiting further generation of electron beams. The reaction time is given by the length of the accelerator, which is ~250 m. Details on the operation modes are described in [17].

6. Summary

The laser system that drives the photo injector of FLASH was upgraded in 2009. This laser generates pulse trains consisting of up to 800 or up to 2400 individual micropulses at 1 MHz and 3 MHz repetition rate in the train, respectively. At the output of the laser system, these pulses are transferred to 262 nm wavelength (UV). This wavelength is required for the Cesium Telluride cathodes of the photo injector of the FLASH linac.

The available energy of the individual ultraviolet pulses of the trains amounts to 13 µJ and 36 µJ at 3 MHz and 1 MHz repetition rate in the train, respectively. These energy values are by far sufficient for producing bunches of 0.5 nC and 3 nC charge respectively with the present FLASH photo injector.

The ultraviolet output pulses of the train are synchronized to the RF of the FLASH linac with better than 100 fs accuracy. Theses individual pulses of the train have a nearly Gaussian shape. Their duration depends on the laser oscillator being used for seeding the amplifier chain. With the oscillator of 54 MHz round-trip frequency, the pulse duration is 13 ps (FWHM) for the 3 MHz mode and ≥15 ps for the larger pulse energy obtained at 1 MHz repetition rate.

#153463 - $15.00 USD Received 25 Aug 2011; revised 16 Oct 2011; accepted 21 Oct 2011; published 8 Nov 2011

The amplifying elements of the system are Nd:YLF laser rods that are pumped by fiber-coupled semiconductor diodes. Compared to the flashlamp-pumped laser previously used at FLASH, the new diode-pumped system has several advantages. First, the pump diodes allow for an improved stability of the laser pulse parameters resulting in an overall stability of the charge of the generated electron bunches of 1% (rms). Second, maintaining the laser was strongly simplified: The previously required periodic exchange of the flashlamps after several weeks of operation is not required anymore as the lifetime of the pump diodes exceeds 10^5 hours. Apart from that, this long lifetime also contributes to an improvement of the overall stability of the system. Finally, pumping the laser with diodes allows for a more compact design and a reduced size of the laser compared with the flashlamp-pumped version.

The described laser system is fully remote-controlled by an embedded VME computer running the DOOCS control system [18]. Special care has been taken to simplify the use of the laser and its control program as much as possible.

For all these reasons, the present laser is particularly well suited for driving the photo injector of FLASH at DESY Hamburg in daily operation.

An important limit of the described laser concerns the shape of the generated pulses. The version of the laser presently installed at FLASH generates trains of pulses with a Gaussian shape only. As it has been shown by recent investigations, other pulse shapes in both temporal and spatial dimensions can be applied to improve the emittance of the electron beam significantly [4,19]. To overcome this limit, we are working on generating pulses with a programmable shape [15,20]. Furthermore, we are going to increase the repetition rate in the generated pulse trains to 4.5 MHz. In short, we intend to further extend the capabilities of the laser system that it can finally serve as the drive laser for the photo injector of the upcoming European XFEL at DESY Hamburg.

Acknowledgments

We also would like to thank the engineers H. Willert, G. Koss, W. Liebich, F. Kroll, H. Benedix, K. Klose and T. Schulz for their creative work during the development of the laser. The authors have benefited from many valuable discussions with colleagues from the MBI and DESY, in particular M. Kalashnikov, J. Bähr, K. Rehlich, O. Henzler, G. Klemz, F. Stephan, M. Krasilnikov, A. Oppelt, J. Rossbach, and K. Flöttmann. We thank Prof. W. Sandner and U. Gensch for their support of this project.

This work was partially supported by the German Bundesministerium for Education and Science, contract nos. 01SF9982/8 and 05ES4BM1/1.

#153463 - $15.00 USD Received 25 Aug 2011; revised 16 Oct 2011; accepted 21 Oct 2011; published 8 Nov 2011